J Arid Land (2023) 15(6): 724–739
https://doi.org/10.1007/s40333-023-0058-8

Science Press Springer-Verlag

Effects of drought treatment on photosystem II activity in the ephemeral plant *Erodium oxyrhinchum*

CHEN Yingying[1,2], LIN Yajun[1,2], ZHOU Xiaobing[1], ZHANG Jing[1], YANG Chunhong[3,4*], ZHANG Yuanming[1*]

[1] State Key Laboratory of Desert and Oasis Ecology/Key Laboratory of Ecological Safety and Sustainable Development in Arid Lands, Xinjiang Institute of Ecology and Geography, Chinese Academy of Sciences, Urumqi 830011, China;
[2] University of Chinese Academy of Sciences, Beijing 100049, China;
[3] Key Laboratory of Plant Resources and Beijing Botanical Garden, Institute of Botany, Chinese Academy of Sciences, Beijing 100093, China;
[4] Zhejiang Lab, Hangzhou 311121, China

Abstract: Drought is a critical limiting factor affecting the growth and development of plants in arid and semi-arid areas. Photosynthesis, one of the most important physiological processes of plants, can be significantly inhibited by drought. Photosystem II (PSII) is considered the main attack target when photosynthesis is affected by drought. To clarify how PSII components of the ephemeral plant *Erodium oxyrhinchum* (grown in the Gurbantunggut Desert, China) respond to drought treatment, we evaluated the functional activity of PSII by determining chlorophyll fluorescence and gas exchange parameters under different drought treatment levels (control (400 mL), moderate drought (200 mL), and severe drought (100 mL)). Under moderate drought treatment, significant decreases were found in net photosynthetic rate (Pn), effective quantum yield of PSII (Y(II)), relative electron transfer rate of PSII (rETR(II)), oxygen-releasing complex, probability of an absorbed exciton moving an electron into the electron transport chain beyond primary quinone receptor Q_A^- ($\Phi(E_o)$), probability of a trapped exciton moving an electron into the electron transport chain beyond primary quinone receptor Q_A^- ($\psi(E_o)$), and performance index of PSII (PI_{abs}). Compared to control treatment, marked increases were observed in water use efficiency (WUE), relative variable fluorescence at the J step (V_J), initial fluorescence (F_o), and dissipated energy per active reaction center (DI_o/RC) under moderate drought treatment, but there were no substantial changes in semi-saturated light intensity (I_K), active reaction centers per cross-section (RC/CS), and total performance index of PSII and PSI (PI_{total}, where PSI is the photosystem I). The changes of the above parameters under severe drought treatment were more significant than those under moderate drought treatment. In addition, severe drought treatment significantly increased the absorbed energy per active reaction center (ABS/RC) and trapping energy per active reaction center (TR_o/RC) but decreased the energy transmission connectivity of PSII components, RC/CS, and PI_{total}, compared to moderate drought and control treatments. Principle component analysis (PCA) revealed similar information according to the grouping of parameters. Moderate drought treatment was obviously characterized by RC/CS parameter, and the values of F_o, V_J, ABS/RC, DI_o/RC, and TR_o/RC showed specific reactions to severe drought treatment. These results demonstrated that moderate drought treatment reduced the photochemical activity of PSII to a certain extent but *E. oxyrhinchum* still showed strong adaptation against drought treatment, while severe drought treatment seriously damaged the structure of PSII. The results of

*Corresponding author: YANG Chunhong (E-mail: yangch@ibcas.ac.cn); ZHANG Yuanming (E-mail: zhangym@ms.xjb.ac.cn)
The first and second authors contributed equally to this work.
Received 2022-11-19; revised 2023-03-08; accepted 2023-03-20

this study are useful for further understanding the adaptations of ephemeral plants to different water conditions and can provide a reference for the selection of relevant parameters for photosynthesis measurements of large samples in the field.

Keywords: chlorophyll fluorescence; drought treatment; electron transport; photosynthesis; photosystem II; *Erodium oxyrhinchum*; Gurbantunggut Desert

Citation: CHEN Yingying, LIN Yajun, ZHOU Xiaobing, ZHANG Jing, YANG Chunhong, ZHANG Yuanming. 2023. Effects of drought treatment on photosystem II activity in the ephemeral plant *Erodium oxyrhinchum*. Journal of Arid Land, 15(6): 724–739. https://doi.org/10.1007/s40333-023-0058-8

1 Introduction

Ephemeral plants, which are widely distributed in the Gurbantunggut Desert of China (Duan et al., 2017), are usually annual herbs with short growth cycle and high photosynthetic rate (Qiu et al., 2007; Tu et al., 2016; Wu et al., 2020). As drought sensitive species, ephemeral plants are sensitive to water availability; they can quickly complete their life cycle by using ice and snow melting water in winter and precipitation in early spring before the arrival of dry and hot summer (Zhang and Chen, 2002).

Lan et al. (2008) reported that the adaptation of annual early spring ephemeral plants to the arid environment occurs not just through the specialization of internal structures, but also due to their unique physiological characteristics within their short life history. For example, adaptations against drought can be achieved by simply adjusting leaf movements to reduce leaf temperature and water loss through respiration (Forseth and Ehleringer, 1980; Yuan and Tang, 2010a) or by regulating leaf osmotic potential (Forseth and Ehleringer, 1982; Zhou et al., 2010). Some studies have shown that a reduction in condensate water can decrease the transpiration and net photosynthetic rate (*Pn*), but have no obvious impact on the intercellular CO_2 concentration and water use efficiency (WUE), reflecting a stable water utilization strategy for ephemeral plants (Gong et al., 2017; Liu et al., 2018). Zhou et al. (2010) also demonstrated that drought significantly reduces *Pn* in *Malcolmia africana.* A recent study showed that increasing precipitation can promote the photosynthetic efficiency in ephemeral plants (Zhang et al., 2022). Ephemeral plants have evolved distinct adaptative mechanisms under drought conditions in the desert environment; however, the specific photosynthetic responses to drought remain unclear, especially for photosystem II (PSII).

PSII activity is a sensitive indicator to evaluate the external environmental stress for plants (Kalaji et al., 2016). PSII is considered the primary target of attack in photosynthesis under external environmental stress (Liu et al., 2018). Chlorophyll fluorescence can be used to quantify the energy distribution dynamics of PSII and determine the photosynthetic physiological status of plants (Krause and Weis, 1991). Furthermore, the rapid chlorophyll fluorescence induction kinetic curve (OJIP) can reflect the changes in primary photochemical reactions of PSII, as well as the structure and state of the photosynthetic mechanisms (Strasser et al., 1995, 2004). Drought stress strongly alters the shape of the OJIP, which manifests its effects on plant physical responses in various patterns and forms the induction transient (Li, 2007; Kalaji et al., 2016). It is accepted that the L (0.01–0.30 ms), K (0.01–2.00 ms), H (2.00–30.00 ms), and G (30.00–1000.00 ms) bands can be used to represent different transient stages to analyze the changes in each stage of the OJIP in more detail (Strasser et al., 2004; Stirbet and Govindjee, 2012). Based on the thylakoid membrane energy flux theory, Strasser et al. (2004) developed a data processing method for the OJIP (i.e., the JIP test). The analysis of the energy flux, flux ratio per reaction center, and unit leaf cross-section in the JIP test can provide detailed information on the redox state of PSII (Strasser et al., 2010; Stirbet and Govindjee, 2011; Kalaji et al., 2016). Chlorophyll fluorescence has been widely used to analyze the response of PSII to drought stress (Zivcak et al., 2013; Zhou et al., 2019; Bano et al., 2021).

In the Gurbantunggut Desert, *Erodium oxyrhinchum* dominates the layer of ephemeral plants

and is limited by water during the growing period (Wang et al., 2006; Li et al., 2020; Mu et al., 2021). In this paper, *E. oxyrhinchum* was selected to investigate the effects of drought treatment on its PSII activity. At present, some researchers have studied the effects of precipitation on the isochronous germination of *E. oxyrhinchum* (Liu et al., 2021), the influences of snow on its seedling growth (Wu et al., 2018), and the impacts of water and nitrogen additions on its life history (Chen et al., 2019). In terms of photosynthesis, the impacts of precipitation on chlorophyll fluorescence (Zhang et al., 2022) and the influences of biological soil crusts on photosynthetic characteristics (Zhuang and Zhang, 2017) are the only topics that have been studied so far. There are few studies on the photosynthesis of *E. oxyrhinchum* under drought treatment, especially with respect to PSII. Thus, a drought simulation experiment of *E. oxyrhinchum* was designed in this study. The response characteristics of leaf photosynthesis and chlorophyll fluorescence of *E. oxyrhinchum* to drought treatment were analyzed to clarify how the components of PSII respond to drought treatment. This study can provide a theoretical basis for improving the stress resistance and photosynthetic efficiency of *E. oxyrhinchum*, as well as other ephemeral plants in the Gurbantunggut Desert.

2 Materials and methods

2.1 Plant materials and experimental design

The experiment was carried out in a sunlight room with natural sunlight and indoor temperature of 25°C from April to June of 2021 in Xinjiang Institute of Ecology and Geography, Chinese Academy of Sciences, Urumqi, China. Seeds of *E. oxyrhinchum* and the cultivated sand soil were collected from the Gurbantunggut Desert (44°11′–46°20′N, 84°31′–90°00′E) in early June 2020. The collected seeds were dried with natural air and then preserved in the laboratory. The outer seed coat was cut with a plant-dissecting knife to break the physical dormancy of seeds before sowing.

We set the control treatment based on the average precipitation amount and precipitation frequency during the growing season of 2017–2019 in the Gurbantunggut Desert reported by Min (2020). We further set two drought treatments, with 50% of the control treatment as the moderate drought and 25% of the control treatment as the severe drought. The actual cumulative precipitation from March to June was calculated to be close to 50.0 mm, and the precipitation frequency was 6 d. That is, about 3.3 mm of precipitation occurred every 6 d. Based on the volume of the flowerpot (height of 25 cm and diameter of 17 cm), we finally set the irrigation volume as follows: 400 mL of water for the control treatment, 200 mL for the moderate drought treatment, and 100 mL for the severe drought treatment for every 6 d. Each drought treatment had 5 replicates, with a total of 15 flowerpots. Approximately 7 or 8 seeds were sown in each flowerpot. In the early stage, seeds were sufficiently watered every 6 d using an artificial sprayer, with about 3.3 mm (400 mL as the control) tap water totally on each flowerpot. Once the seeds have germinated, 3 robust seedlings were kept in each flowerpot and the excess seedlings were pulled out. After one and a half months of growth, when the plants reached the leaf-expansion stage, drought treatment lasted for 12 d, watering every 6 d. Measurements of parameters were conducted during this period (i.e., after one and a half months of growth).

2.2 Leaf gas exchange measurements

Leaf gas exchange parameters were measured with Li-6400 (Li-COR Inc., Lincoln, Nebraska, USA) on a sunny day from 09:00 to 12:00 (LST) in the morning. The measured parameters included *Pn*, transpiration rate (*Tr*), stomatal conductance (*Gs*), and WUE (which was calculated from the ratio of *Pn* to *Tr*), and the values were recorded after stabilization for 10.00 min. The cuvette settings were as follows: 1500.00 μmol photons/(m^2·s) for photosynthetic photon flux density (PPFD), 500.00 mmol/s for flow rate, and 400.00 mmol/mol for CO_2, and the cuvette fan was set to fast mode. After measurements, the leaves were photographed using the software Image J (Rawak Software, Carlsbad, CA, USA) to determine the leaf areas. Then, the parameters of *Pn* (μmol/(m^2·s)), *Tr* (mmol/(m^2·s)), and *Gs* (mmol/(m^2·s)) can be obtained by the measuring

instrument and software directly. Each drought treatment is an average of five replicates.

2.3 Chlorophyll fluorescence measurements

We adjusted the plants dark-adapted for 30.00 min before measurements using a portable PAM-2500 fluorometer (Heinz Walz GmbH, Effeltrich, Germany), according to the methods of Schreiber et al. (1986). The measured light intensity was 0.15 μmol photons/(m^2·s), the saturated pulse intensity was 10,000.00 μmol photons/(m^2·s) for 0.80 s, and the pulse interval was 20.00 s. The gradient of light intensity was set as 0.00, 5.00, 93.00, 201.00, 514.00, 877.00, 1381.00, 1647.00, 1967.00, 2362.00, and 2862.00 μmol photons/(m^2·s); in turn, the duration of the applied light for each light intensity was 300.00 s, and the instrument measurement software can automatically calculate the effective quantum yield of PSII (Y(II)), photochemical quenching (qP), closure degree of PSII (1–qP), quantum yield of regulated energy dissipation in PSII ($Y(NPQ)$), and quantum yield of nonregulated energy dissipation in PSII ($Y(NO)$). The fluorescence parameters were calculated as follows (Krall and Edwards, 1992; Kramer et al., 2004; Klughammer and Schreiber, 2008):

$$Y(\mathrm{II}) = (Fm' - Fs) / Fm', \tag{1}$$

$$qP = (Fm' - Fs) / (Fm' - F_o'), \tag{2}$$

$$Y(NPQ) = Fm / Fm' - 1, \tag{3}$$

$$Y(NO) = Fs / Fm, \tag{4}$$

where Fm and Fm' represent the maximal fluorescence from dark-adapted and light-adapted leaves, respectively; F_o' represents the minimal fluorescence from light-adapted leaves; and Fs represents the steady state fluorescence yield from light adaptation.

The fast light response curve of relative electron transfer rate of PSII (rETR(II); μmol/(m^2·s)) was fitted using the equation described by Platt et al. (1980). The gradient of light intensity was set as 0.00, 5.00, 45.00, 93.00, 145.00, 201.00, 385.00, 514.00, 877.00, 1115.00, 1381.00, 1647.00, 1967.00, 2362.00, and 2862.00 μmol photons/(m^2·s); in turn, the duration of the applied light for each light intensity was 30.00 s, and the instrument measurement software can automatically calculate the rETR(II). The relevant parameters obtained from the fit equation were the maximum electron transfer rate ($\mathrm{ETR_{max}}$; μmol/(m^2·s)), semi-saturated light intensity (I_K; μmol/(m^2·s)), initial slope of the fast light response curve (α), and photosynthetically active radiation (PAR; μmol/(m^2·s)). Each treatment is an average of five replicates.

$$r\,\mathrm{ETR(II)} = Y(\mathrm{II}) \times \mathrm{PAR} \times 0.84 \times 0.5, \tag{5}$$

$$I_K = \mathrm{ETR_{max}} / \alpha. \tag{6}$$

2.4 Rapid chlorophyll fluorescence measurements

We monitored the rapid chlorophyll fluorescence induction kinetics *in situ* artificially with plant efficiency analyzer (HandyPEA, Hansatech Instruments Ltd., Norfolk, UK), according to the method described by Strasser et al. (2004). After dark adaptation for 30.00 min, the fluorescence induction kinetics of plants were measured. Red light (wavelength of 650.00 nm and light intensity of 3500.00 μmol photons/(m^2·s)) was used to induce chlorophyll fluorescence. Measurement for each drought treatment is an average of five replicates. All fluorescence values were selected from the period from 10.00 μs to 2.00 s. A typical OJIP resembles the different fluorescence states: the first rise from the origin is denoted as "O", which ascends to an intermediate state "K" step (at 0.30 ms) and "J" step (at 2.00 ms), followed by a second slower rise involving a second intermediate state "I" step (at 30.00 ms), while the "P" step is the maximum fluorescence measured. The OP, OJ, OK, JI, and IP stages were standardized to further analyze the fluorescence dynamic curves. The abscissa representing time was changed to a logarithmic coordinate to present the OJIP. Then, we analyzed the OJIP fluorescence transients according to the JIP test (Strasser et al., 2000), in which data were also visualized by generating radar plots of bioenergetic fluxes.

2.5 Statistical analysis

Preliminary data statistics were performed in Excel, then one-factor analysis of variance (ANOVA) was used to analyze the differences in SPSS 28.0 (IBM, Almonte, New York, USA). The data are shown as the means and standard deviations, and the Duncan's test was used to compare means (P<0.05). We explored the variability of the measured parameters and their correlations by principal component analysis (PCA). The axis with the characteristic value greater than 1 was selected as the principal component axis. Graphs were constructed using OriginPro 2021 software (OriginLab, Northampton, USA).

3 Results

3.1 Effects of different drought treatment levels on phenotype and leaf gas exchange parameters of *E. oxyrhinchum*

The plants under severe drought treatment showed a distinct difference in phenotype compared to those under control and moderate drought treatments, and there was no noteworthy difference between plants under control and moderate drought treatments (Fig. 1). Parameters of *Pn*, *Gs*, and *Tr* decreased significantly with increasing drought level. *Pn* under moderate and severe drought treatments decreased by 47.82% and 86.92%, respectively, and the corresponding declines were 49.11% and 86.82% for *Gs* and 61.77% and 92.04% for *Tr*, compared with control treatment (P<0.05; Fig. 2a–c). However, an opposite trend was observed for WUE, which increased by 36.51% and 64.19% under moderate and severe drought treatments, respectively, compared with control treatment (P<0.05; Fig. 2d).

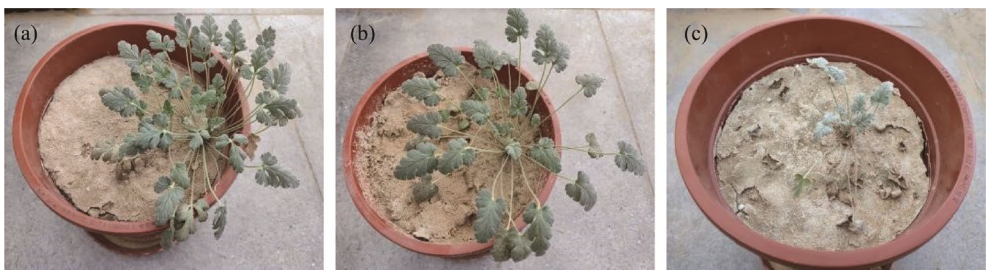

Fig. 1 Phenotype of *Erodium oxyrhinchum* grown under different drought treatment levels. (a), control treatment; (b), moderate drought treatment; (c), severe drought treatment.

3.2 Effects of different drought treatment levels on the response curve of chlorophyll fluorescence in *E. oxyrhinchum*

When PPFD was lower than 500.00 μmol photons/(m^2·s), parameters of Y(II), Y(*NPQ*), 1–*qP*, and Y(*NO*) did not change significantly regardless of drought treatment. When PPFD increased to greater than 500.00 μmol photons/(m^2·s), the trend of Y(II) declined, but Y(*NPQ*), Y(*NO*), and 1–*qP* observably improved (Fig. 3). Y(II) and Y(*NO*) decreased with increasing drought treatment level (Fig. 3a and d), while Y(*NPQ*) and 1–*qP* continued to increase (Fig. 3b and c).

The parameter of *r*ETR(II) increased with increasing PPFD and decreased with increasing drought treatment level (Fig. 4a). The values of ETR_{max} and α under moderate and severe drought treatments were significantly lower than those under control treatment. Nevertheless, there was no significant difference between moderate and severe drought treatments (P<0.05; Fig. 4b and c). ETR_{max} reached 589.66 (±64.66), 195.40 (±26.30), and 137.25 (±25.69) μmol/(m^2·s) under control, moderate drought, and severe drought treatments, respectively, after illumination (Fig. 4b). Compared with control treatment, α parameter respectively decreased by 59.72% and 65.40% under moderate and severe drought treatments (Fig. 4c), while I_K decreased by 11.39% and 65.95%, respectively (Fig. 4d). I_K showed little difference between control and moderate drought treatments (P>0.05), and both were prominently higher than that under severe drought treatment (P<0.05; Fig. 4d).

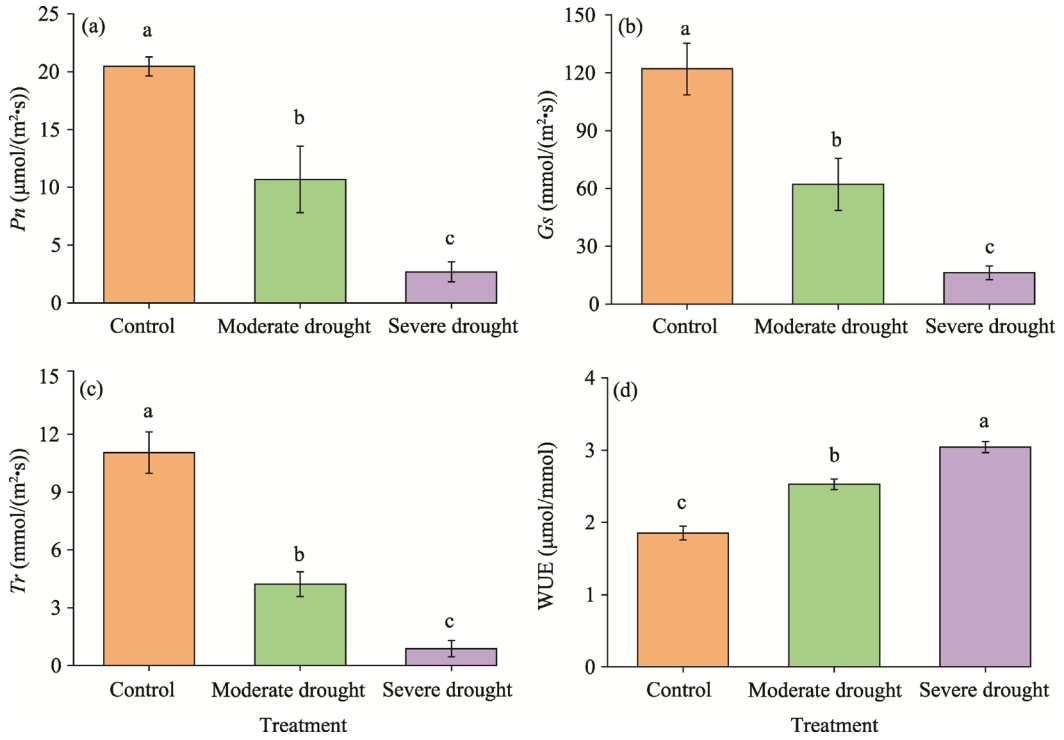

Fig. 2 Leaf gas exchange parameters of *E. oxyrhinchum* under different drought treatment levels. (a), net photosynthetic rate (*Pn*); (b), stomatal conductance (*Gs*); (c), transpiration rate (*Tr*); (d), water use efficiency (WUE). Different lowercase letters indicate significant differences among drought treatments at $P<0.05$ level based on the Duncan's test. Bars mean standard deviations.

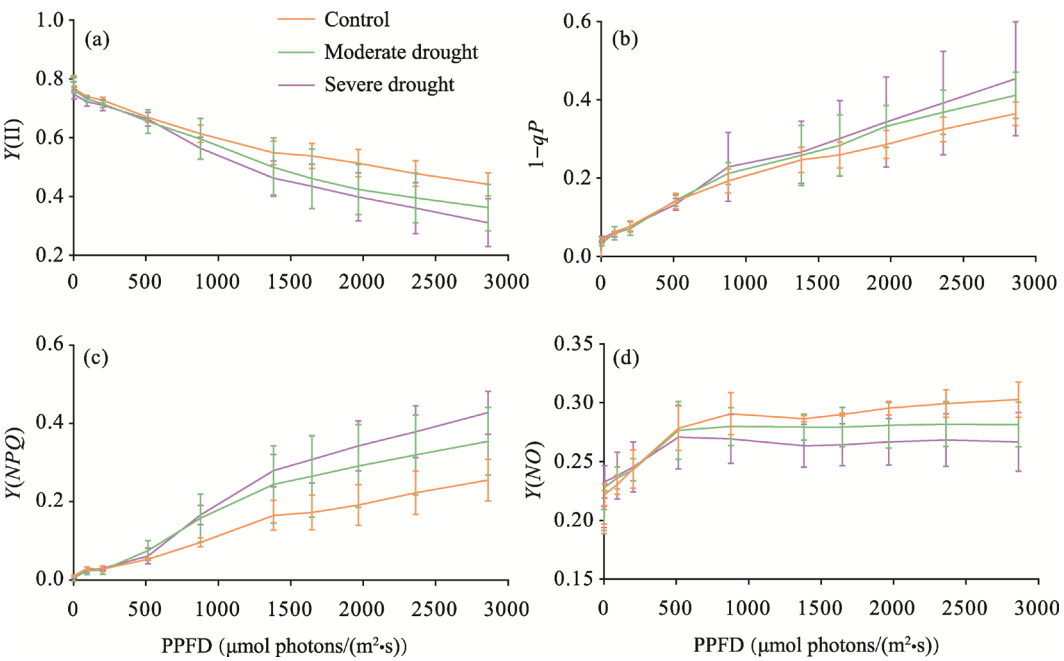

Fig. 3 Light response curves of *E. oxyrhinchum* under different drought treatment levels. (a), effective quantum yield of photosystem II (PSII) (*Y*(II)); (b), closure degree of PSII (1–*qP*); (c), quantum yield of regulated energy dissipation in PSII (*Y*(*NPQ*)); (d), quantum yield of nonregulated energy dissipation in PSII (*Y*(*NO*)). PPFD, photosynthetic photon flux density. Bars mean standard deviations.

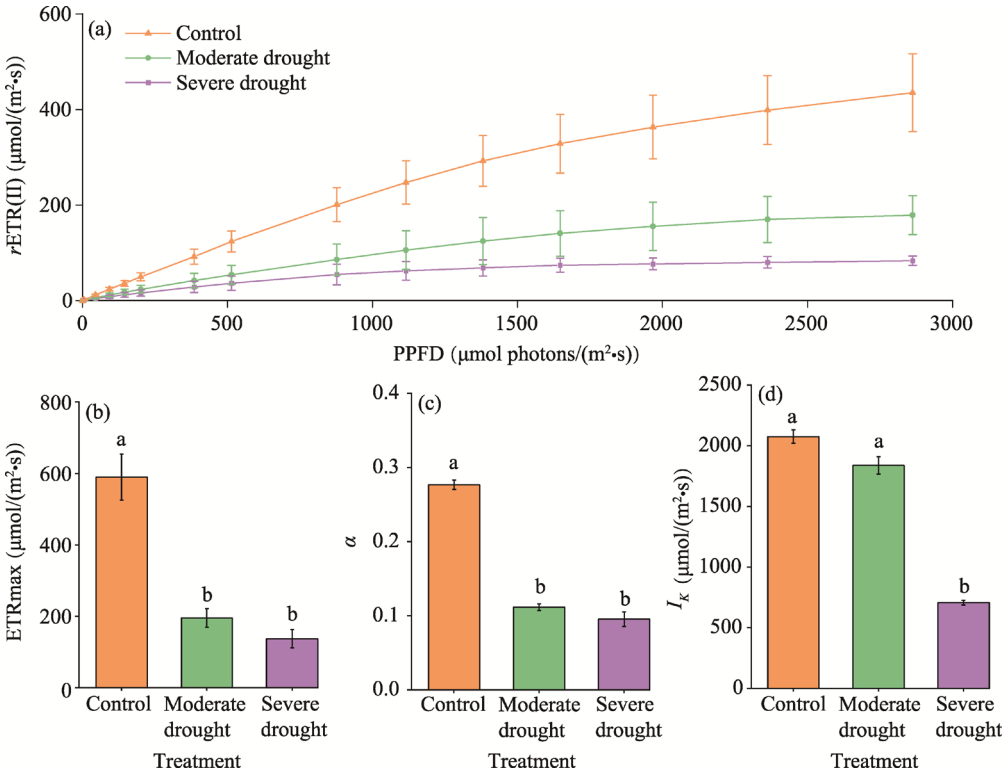

Fig. 4 Fitted light response curves of (a) relative electron transfer rate of PSII (*r*ETR(II)), (b) maximum electron transfer rate (ETR_{max}), (c) initial slope of the fast light response curve (α), and (d) semi-saturated light intensity (I_K) of *E. oxyrhinchum* under different drought treatment levels. Different lowercase letters indicate significant differences among drought treatments at $P<0.05$ level based on the Duncan's test. Bars mean standard deviations.

3.3 Effects of different drought treatment levels on the OJIP fluorescence transients of *E. oxyrhinchum*

Figure 5 shows the OJIP of *E. oxyrhinchum* under different drought treatment levels. In general, *E. oxyrhinchum* under moderate and severe drought treatments showed a similar curve trend with that under control treatment (Fig. 5a). Thus, the OJIP fluorescence transients were subjected to double normalization in stages O–P. The relative fluorescence values of "J" step and "I" step were obviously increased (Fig. 5b). To further reveal the details in different stages, we double-normalized O–J, O–K, J–I, and I–P (Fig. 5c, e, g, and i) to visualize the K, L, H, and G bands (Fig. 5d, f, h, and j). With increasing drought treatment level, the obvious positive K band showed that the oxygen-releasing complex was inactivated. The L band was positive under severe drought treatment, indicating that the energy transmission connectivity of PSII components was reduced, and the opposite was also true under moderate drought treatment. The positive H band decreased the relative size of the plastoquinone (PQ) pool, especially under severe drought treatment. The G band was positive under moderate drought and severe drought treatments, indicating that the acceptor pool of photosystem I (PSI) became relatively small.

The photosynthetic process of each step can be revealed by the JIP test based on the OJIP fluorescence transients. In this study, drought treatment altered several selected characteristics and some important JIP test parameters. As the level of drought treatment increased, the minimum fluorescence (F_o), relative variable fluorescence at the J step (V_J), and dissipated energy per active reaction center (DI_o/RC) significantly increased, while the probability of a trapped exciton moving an electron into the electron transport chain beyond primary quinone receptor Q_A^- ($\psi(E_o)$), probability of an absorbed exciton moving an electron into the electron transport chain beyond primary quinone receptor Q_A^- ($\Phi(E_o)$), and performance index of PSII (PI_{abs}) markedly

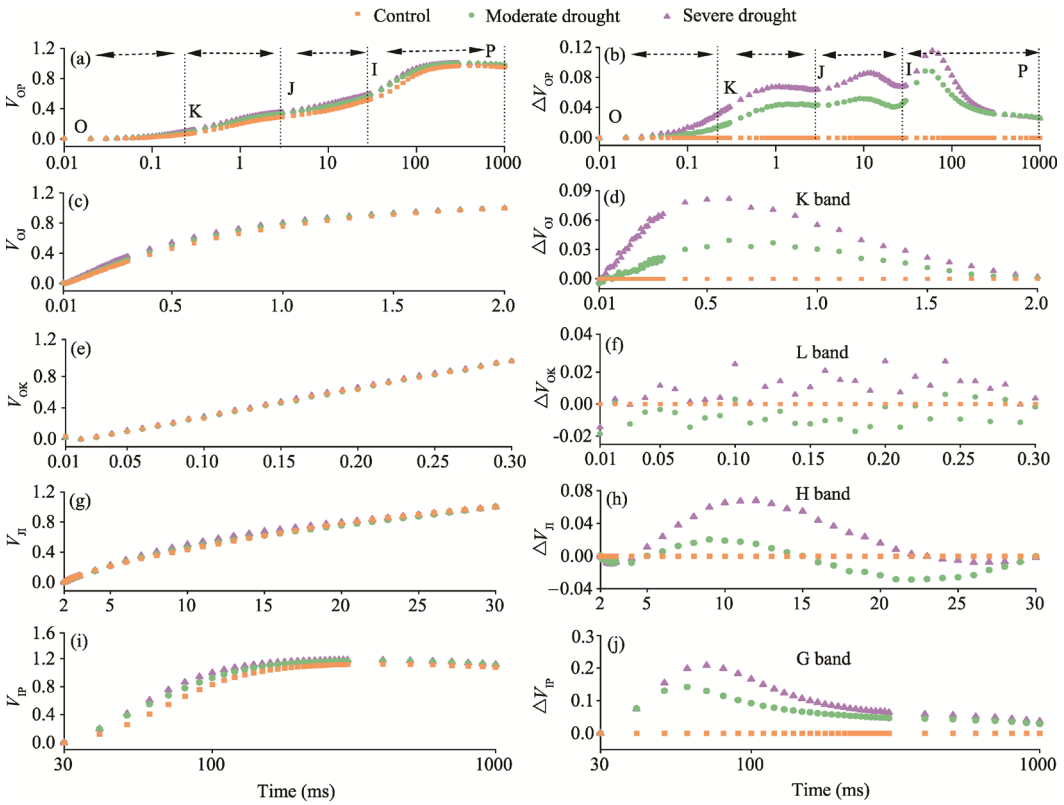

Fig. 5 Rapid chlorophyll fluorescence induction kinetics curve (OJIP) of *E. oxyrhinchum* under different drought treatment levels. The first rise from the origin is denoted as "O", which ascends to an intermediate state "K" step (at 0.30 ms) and "J" step (at 2.00 ms), followed by a second slower rise involving a second intermediate state "I" step (at 30.00 ms), while the "P" step is the maximum fluorescence measured. (a), relative variable fluorescence at stages O–P (V_{OP}); (b), relative variable fluorescence after normalization at stages O–P (ΔV_{OP}); (c), relative variable fluorescence at stages O–J (V_{OJ}); (d), relative variable fluorescence of K band after normalization at stages O–J (ΔV_{OJ}); (e), relative variable fluorescence at stages O–K (V_{OK}); (f), relative variable fluorescence of L band after normalization at stages O–K (ΔV_{OK}); (g) relative variable fluorescence at stages J–I (V_{JI}); (h), relative variable fluorescence of H band after normalization at stages J–I (ΔV_{JI}); (i) relative variable fluorescence at stages I–P (V_{IP}); (j), relative variable fluorescence of G band after normalization at stages I–P (ΔV_{IP}). Relative variable fluorescence was calculated as $V_t=(F_t-F_o)/(F_m-F_o)$ (where, F_o is the minimum fluorescence; F_m is the maximum fluorescence; and F_t is the fluorescence at t time) and relative variable fluorescence after normalization was determined as $\Delta V_t=V_t-V_{control}$ (where V_t is the relative variable fluorescence at t time; and $V_{control}$ is the relative variable fluorescence at t time under control treatment).

decreased (P<0.05; Fig. 6). Drought treatment decreased the maximal photochemical efficiency (Fv/Fm, where Fv is the variable fluorescence) and the size of the PQ pool on the PSII receptor side (S_m) (P<0.05). The absorbed energy per active reaction center (ABS/RC) and trapping energy per active reaction center (TR_o/RC) increased under severe drought treatment, while the active reaction center per cross-section (RC/CS) significantly decreased (P<0.05). However, the electron flux from the active reaction center to the PSI acceptor side (RE_o/RC) and the probability of an electron being transported from reduced PQ to the electron acceptor side of PSI (δR_o) showed no notable changes under moderate and severe drought treatments (P>0.05), compared with control treatment. The total performance index of PSII and PSI (PI_{total}) under moderate drought treatment was not significantly different with that under control and severe drought treatments, but it was significantly lower under severe drought treatment than under control treatment (Fig. 6).

3.4 PCA on gas exchange and chlorophyll fluorescence of *E. oxyrhinchum* under different drought treatment levels

Gas exchange and chlorophyll fluorescence parameters of *E. oxyrhinchum* under drought

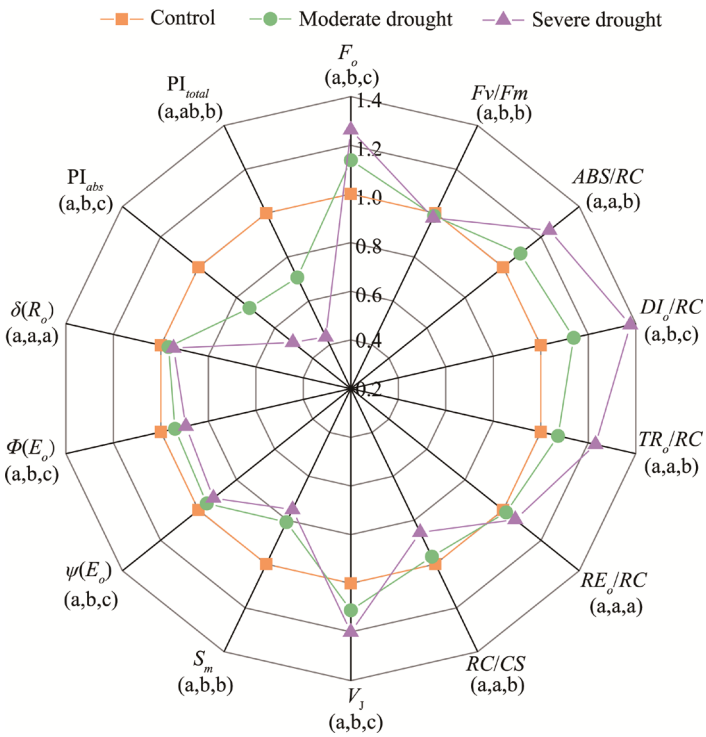

Fig. 6 Data processing method for the OJIP (JIP test) parameters of *E. oxyrhinchum* under different drought treatment levels. The rapid chlorophyll fluorescence parameters under control treatment were taken as 1 and the rapid chlorophyll fluorescence parameters under moderate drought and severe drought treatments were expressed as the proportion of that under control treatment. Different lowercase letters in the parentheses indicate significant differences at $P<0.05$ level based on the Duncan's test. *Fv*/*Fm*, the maximal photochemical efficiency (where *Fv* is the variable fluorescence); *ABS*/*RC*, absorbed energy per active reaction center; DI_o/RC, dissipated energy per active reaction center; TR_o/RC, trapping energy per active reaction center; RE_o/RC, electron flux from the active reaction center to the PSI acceptor side; *RC*/*CS*, active reaction centers per cross-section; V_J, relative variable fluorescence at the J step; S_m, the size of the plastoquinone (PQ) pool on the PSII receptor side; $\psi(E_o)$, probability of a trapped exciton moving an electron into the electron transport chain beyond primary quinone receptor Q_A^-; $\Phi(E_o)$, probability of an absorbed exciton moving an electron into the electron transport chain beyond primary quinone receptor Q_A^-; δR_o, probability of an electron being transported from reduced PQ to the electron acceptor side of photosystem I (PSI); PI_{abs}, the performance index of PSII; PI_{total}, the total performance index of PSII and PSI.

treatments were analyzed by PCA (Table 1). The parameters of *E. oxyrhinchum* under severe drought treatment had a negative distribution and were different from those under control and moderate drought treatments, which showed positive distributions. The parameters under moderate drought treatment slightly overlapped with those under control treatment and were between those under control and severe drought treatments (Fig. 7). Most of the variance (90.3%) was explained by the first two principal components (PCs). The first PC (PC1), which reflected 83.0% of the total variance, including parameters of F_o, *Fv*/*Fm*, *ABS*/*RC*, DI_o/RC, TR_o/RC, $\psi(E_o)$, $\Phi(E_o)$, V_J, S_m, *Pn*, PI_{total}, PI_{abs}, and I_K (Table 1; Fig. 7). The second PC (PC2), which was characterized by a higher load on *RC*/*CS*, explained 7.3% of the total variance (Table 1; Fig. 7). Parameters of PI_{abs}, PI_{total}, *Fv*/*Fm*, *Pn*, S_m, $\psi(E_o)$, $\Phi(E_o)$, I_K, and *RC*/*CS* were positively correlated with each other, but they were negatively correlated with F_o, V_J, *ABS*/*RC*, DI_o/RC, and TR_o/RC (Fig. 7).

4 Discussion

Different drought treatment levels have various effects on photosynthetic rate. Under mild and moderate drought treatments, the restriction of CO_2 diffusion from atmosphere to chloroplast

Table 1 Contributions of different chlorophyll fluorescence and gas exchange parameters of *E. oxyrhinchum* to the total variance of principal components (PCs)

Parameter	PC1	PC2
F_o	–0.2849#	–0.1477
Fv/Fm	0.2804#	–0.0230
ABS/RC	–0.2799#	0.1460
DI_o/RC	–0.2792#	0.1512
TR_o/RC	–0.2756#	0.1429
$\psi(E_o)$	0.2847#	–0.0581
$\Phi(E_o)$	0.2840#	–0.0241
PI_{abs}	0.2842#	0.0401
PI_{total}	0.2609#	–0.0174
V_J	–0.2871#	–0.0095
S_m	0.2523#	0.0939
Pn	0.2858#	0.1200
RC/CS	0.0732	0.9280#
I_K	0.2537#	–0.1506

Note: PC1, the first principal component; PC2, the second principal component; #, parameters with high contribution; F_o, the minimum fluorescence; Fv/Fm, the maximal photochemical efficiency (where Fv is the variable fluorescence and Fm is the maximum fluorescence); ABS/RC, absorbed energy per active reaction center; DI_o/RC, dissipated energy per active reaction center; TR_o/RC, trapping energy per active reaction center; $\psi(E_o)$, probability of a trapped exciton moving an electron into the electron transport chain beyond primary quinone receptor Q_A^-; $\Phi(E_o)$, probability of an absorbed exciton moving an electron into the electron transport chain beyond primary quinone receptor Q_A^-; PI_{abs}, the performance index of photosystem II (PSII); PI_{total}, the total performance index of PSII and photosystem I (PSI); V_J, relative variable fluorescence at the "J" step; S_m, size of plastoquinone (PQ) pool in PSII receptor side; Pn, net photosynthetic rate; RC/CS, active reaction centers per cross-section; I_K, semi-saturated light intensity.

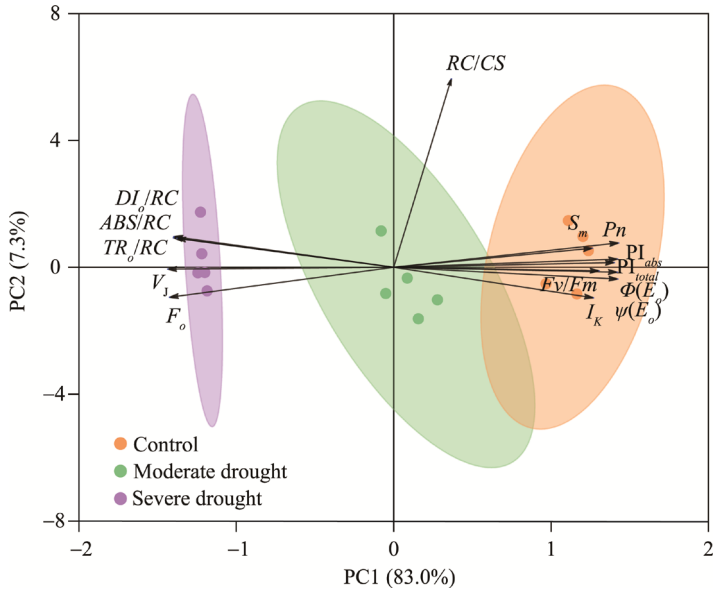

Fig. 7 Biplot of principal component analysis (PCA) showing the separation of the chlorophyll fluorescence and gas exchange parameters of *E. oxyrhinchum* under different drought treatment levels. PC1, the first principal component; PC2, the second principal component.

carboxylation site is the main reason for the decrease of photosynthetic rate, which is known as stomatal limitation (Farquhar and Sharkey, 1982; Pinheiro and Chaves, 2011; Wang et al., 2018). With the aggravation of drought, rubisco activity decreases and electron transport complex function is impaired, further reducing photosynthetic rate, which is usually a nonstomatal limitation (Farquhar and Sharkey, 1982; Wang et al., 2018; Wang et al., 2022). *Gs* decreased with increasing drought intensity in this study. The main reasons for the decrease of *Pn* under moderate

drought treatment may be stomatal factors. The nonstomatal restriction under severe drought treatment possibly led to a reduction in *Pn*. This is consistent with the results of alpine meadow plants in response to drought (Ma et al., 2021). Compared to control treatment, the *Tr* values of *E. oxyrhinchum* under moderate drought and severe drought treatments were significantly lower and may also be one of the causes for the lower *Pn*. The lower *Tr* can result in higher leaf temperature, stronger photoinhibition, and lower photosynthetic capacity (Wang et al., 2022). Furthermore, the reduction in leaf area to reduce transpiration has also been considered a survival adaptation strategy against drought stress. Leaf area plasticity is regarded as an essential strategy for controlling WUE (Talbi et al., 2020). Higher WUE under drought stress is an essential means to obtain stronger drought resistance (Xu et al., 2017; Wang et al., 2021). In our study, WUE and phenotype significantly differed between control and drought treatments. The results showed that to prevent excessive water loss and ensure full utilization of water, the decrease in the photosynthesis of *E. oxyrhinchum* might mainly be controlled by stomata. Through physiological metabolism, the drought tolerance and adaptability of this species can be enhanced to ensure normal growth.

The decrease in photosynthetic capacity further affects the photochemical reaction, leading to more excess excitation energy and photoinhibition damage to PSII (Luo et al., 2016; Fernández-Marín et al., 2020; Wang et al., 2022). In this research, the significant decrease in *Y*(II) showed that the absorbed light through the antenna of PSII reaction centers was less efficient in charge separation. However, *Y*(*NPQ*) was significantly increased to dissipate excess energy and avoid damage to PSII. Additionally, the PCA results showed a significant increase in DI_o/RC. It is notable that *Y*(*NO*) was higher under control treatment than under moderate drought and severe drought treatments. *Y*(*NO*) is related to the light acclimation of photosynthetic mechanisms with high tolerance (Shi et al., 2015). The lower *Y*(*NO*) in *E. oxyrhinchum* under drought treatment may slow the damage from increased light exposure. As described in previous studies, high light stress can be mitigated by priming water deficits in papaya (Vincent et al., 2018) and cashew (Lima et al., 2018). *Y*(*NPQ*) and *Y*(*NO*) are protective mechanisms to maintain normal photosynthesis of plants (Wilson and Ruban, 2020). In this study, both parameters were shown to regulate the energy dissipation of *E. oxyrhinchum*, thus reducing photoinhibition under drought treatment. The reaction of *r*ETR(II) to various light intensity levels was examined to determine the adaptability of plants to strong light under drought treatment. The high I_K under moderate drought treatment indicated a relatively strong tolerance to light. The low value of α implied a decrease in the utilization ability of PSII to capture light energy under drought treatment, eventually reducing the ETR_{max}. These results are consistent with those observed in *Taida Smile* (Wang et al., 2014) and *Sago palm* (Azhar et al., 2021).

In this study, to obtain more in-depth information on light collection and electron transfer of PSII, we analyzed the rapid chlorophyll fluorescence transient by plotting differential curves. The positive K band suggested that drought treatment damaged the oxygen-releasing complex, resulting in an imbalance between electron transport from the oxygen-releasing complex to the acceptor side in PSII (Zhou et al., 2019). The positive L band under severe drought treatment indicated that the energy transmission connectivity between antenna pigment and PSII active reaction center decreased, leading to poor excitation energy utilization as well as lower α value. However, under moderate drought treatment, the energy transmission connectivity of PSII components was improved due to the negative L band (Wang et al., 2018; Zhou et al., 2019). In summary, the oxygen-releasing complex of *E. oxyrhinchum* was the initial target of PSII damage in the early stage of drought. With an increasing drought treatment level, the absorption and dissipation of light energy were reduced by decreasing the energy transmission connectivity of PSII components. The visible H band revealed that the PQ pool comparatively decreased when exposed to drought stress (Paunov et al., 2018). The significant reduction in S_m supported this conclusion. However, under moderate drought treatment, the first half of the H band amplitude was positive and the second half was negative. The G band was positive, reflecting the decrease

in electron acceptor at the end of PSI (Zagorchev et al., 2020). PSI acceptor electron transport may have been inhibited by the increasing drought treatment level. However, the values of RE_o/RC and δR_o showed no significant difference between control and drought treatments, indicating that drought treatment had no distinct impact on PSI. This result suggests that PSII activity is more sensitive to drought treatment than PSI, which is consistent with the findings of *Torreya grandis* under drought stress (Wang et al., 2022).

The JIP test can be used to analyze changes in PSII critical energetic characteristics (Strasser et al., 2004; Redillas et al., 2011). In this study, V_J obviously improved with the increasing drought treatment level, in which the accumulation of Q_A^- relatively increased and the electron transfer capacity on the receptor side was weakened, accompanied by a further decrease in the probability of electron transfer to the electron acceptor beyond Q_A^- in the electron transfer chain (Lu et al., 2020) as well as the obvious decreases in $\Phi(E_o)$ and $\Psi(E_o)$. These factors resulted in significant decreases in Fv/Fm and PI_{abs} values. In addition, under severe drought treatment, the increase in ABS/RC may be due to the inactivation of some PSII reaction centers or the increase in antenna size (Çiçek et al., 2019). These changes were proven by the positive L band and the decrease in RC/CS, which are similar to the results obtained from passion fruit under drought treatment (Gomes et al., 2012). The inactivation of the reaction centers observed when *E. oxyrhinchum* was subjected to severe drought treatment might be an indicator of photoinhibition sensitivity, which is also a downregulation mechanism used to dissipate excess absorbed light. Finally, PI_{abs} and PI_{total} prominently decreased, consistent with the trend of Pn values. However, Fv/Fm did not change significantly under severe drought treatment due to the simultaneous increases in ABS/RC and DI_o/RC (Manaa et al., 2021). This result indicates that PI_{abs} is more sensitive to drought stress than Fv/Fm in photosynthetic mechanisms (Li et al., 2005).

Based on an in-depth analysis of all the data, we selected 14 chlorophyll fluorescence and gas exchange parameters for PCA. The results showed that most parameters were contained in PC1. Hence, PC1 can be considered as a measure of functioning photosynthesis reaction center. The control and severe drought treatments were on the opposing ends of PC1. *E. oxyrhinchum* under control treatment had higher photosynthesis activity and growth rate (Pn, Fv/Fm, PI_{abs}, and PI_{total}) and electron transport ($\psi(E_o)$ and $\Phi(E_o)$). Severe drought treatment resulted in more substantial energy dissipation and inhibited PSII activity (F_o, V_J, ABS/RC, DI_o/RC, and TR_o/RC). The parameters under severe drought treatment were negatively correlated with those under control treatment, which directly showed that the photosynthetic capacity decreased significantly. These results are similar to the effects of temperature and high light on the photochemical efficiency of PSII in soybean-inverted leaves (Wang et al., 2022) and camel thorns (Yue et al., 2020). Moderate drought treatment exhibited the strongest correlation with RC/CS, which slightly overlapped with that under control treatment but was far from that under severe drought treatment, indicating that the photosynthetic capacity of *E. oxyrhinchum* under moderate drought treatment was similar to that under control treatment and significantly higher than that under severe drought treatment.

Water is the most important limiting factor affecting the growth and development of herbaceous plants in the Gurbantunggut Desert (Yuan and Tang, 2010b). *E. oxyrhinchum* completes its life cycle in the early spring by using ice and snow melting water and precipitation. With the advent of the harsh and hot summer, both precipitation amount and the frequency of precipitation decrease (Min, 2020). *E. oxyrhinchum* was gradually subjected to drought treatment, which was first manifested in the inactivation of the oxygen-releasing complex on the donor side of PSII and the accumulation of Q_A^- electrons on the receptor side, thereby reducing electron transfer ability significantly. However, due to the high energy transmission connectivity of PSII components and the more active reaction centers, *E. oxyrhinchum* also had strong light resistance and maintained good growth through heat dissipation. With the extension of drought time and the increasing drought treatment level, the energy transmission connectivity of PSII components and the number of active reaction centers decreased in *E. oxyrhinchum* under severe drought treatment, and Pn significantly decreased, which may promote the transition from vegetative

growth to reproductive growth and thus complete its short life cycle (Eppel et al., 2014; Mu et al., 2021).

5 Conclusions

Drought treatment significantly decreased the photosynthetic performance of *E. oxyrhinchum*. Moderate drought treatment caused oxidative damage, such as oxygen-releasing complex inactivation and the inhibition of electron transport, ultimately significantly reducing PI_{abs}. However, under severe drought treatment, some PSII reaction centers were inactivated and the energy transmission connectivity of PSII components was reduced. These effects eventually led to significant decreases in PI_{abs} and PI_{total}. The damage to the photosynthetic apparatus and the inhibition of electron transport of *E. oxyrhinchum* in arid environments were the reasons for the substantial declines in PSII activity and *Pn*. These results can provide a theoretical basis for understanding the growth adaptability of *E. oxyrhinchum* in the Gurbantunggut Desert.

Acknowledgements

This research was supported by the National Natural Science Foundation of China (U2003214) and the Western Youth Scholars Project of the Chinese Academy of Sciences (2021-XBQNXZ-006).

References

Azhar A, Makihara D, Naito H, et al. 2021. Sago palm (*Metroxylon sagu* Rottb.) response to drought condition in terms of leaf gas exchange and chlorophyll *a* fluorescence. Plant Production Science, 24(1): 65–72.

Bano H, Athar H R, Zafar Z U, et al. 2021. Linking changes in chlorophyll *a* fluorescence with drought stress susceptibility in mung bean [*Vigna radiata* (L.) Wilczek]. Physiologia Plantarum, 172(2): 1244–1254.

Chen Y F, Zhang L W, Shi X, et al. 2019. Life history responses of spring- and autumn-germinated ephemeral plants to increased nitrogen and precipitation in the Gurbantunggut Desert. Science of The Total Environment, 659: 756–763.

Çiçek N, Pekcan V, Arslan Ö, et al. 2019. Assessing drought tolerance in field-grown sunflower hybrids by chlorophyll fluorescence kinetics. Brazilian Journal of Botany, 42: 249–260.

Duan C, Wu L, Wang S M, et al. 2017. Analysis of spatio-temporal patterns of ephemeral plants in the Gurbantunggut Desert over the last 30 years. Acta Ecologica Sinica, 37(8): 2642–2652. (in Chinese)

Eppel A, Shaked R, Eshel G, et al. 2014. Low induction of non-photochemical quenching and high photochemical efficiency in the annual desert plant *Anastatica hierochuntica*. Physiologia Plantarum, 151(4): 544–558.

Farquhar G D, Sharkey T D. 1982. Stomatal conductance and photosynthesis. Annual Review of Plant Physiology, 33: 317–345.

Fernández-Marín B, Gulías J, Figueroa C M, et al. 2020. How do vascular plants perform photosynthesis in extreme environments? An integrative ecophysiological and biochemical story. Plant Journal, 101(4): 979–1000.

Forseth I N, Ehleringer J R. 1980. Solar tracking response to drought in a desert annual. Oecologia, 44(2): 159–163.

Forseth I N, Ehleringer J R. 1982. Ecophysiology of two solar tracking desert winter annuals. Oecologia, 54(1): 41–49.

Gomes M T G, Da Luz A C, Dos Santos M R, et al. 2012. Drought tolerance of passion fruit plants assessed by the OJIP chlorophyll *a* fluorescence transient. Scientia Horticulturae, 142: 49–56.

Gong X W, Lü G H, Welp M, et al. 2017. Water and photosynthetic physiology of *Lappula semiglabra* seedlings under different dew input amounts. Chinese Journal of Ecology, 36(8): 2198–2205. (in Chinese)

Kalaji H M, Jajoo A, Oukarroum A, et al. 2016. Chlorophyll *a* fluorescence as a tool to monitor physiological status of plants under abiotic stress conditions. Acta Physiologiae Plantarum, 38: 102, doi: 10.1007/s11738-016-2113-y.

Klughammer C, Schreiber U. 2008. Complementary PS II quantum yields calculated from simple fluorescence parameters measured by PAM fluorometry and the Saturation Pulse method. PAM Application Notes, 1: 27–35.

Krall J P, Edwards G E. 1992. Relationship between photosystem II activity and CO_2 fixation in leaves. Physiologia Plantarum, 86(1): 180–187.

Kramer D M, Johnson G, Kiirats O, et al. 2004. New fluorescence parameters for the determination of Q_A redox state and

excitation energy fluxes. Photosynthesis Research, 79: 209–218.

Krause G H, Weis E. 1991. Chlorophyll fluorescence and photosynthesis: the basics. Annual Review of Plant Physiology and Plant Molecular Biology, 42: 313–349.

Li D X, Zhang D Y, Zhang L W, et al. 2020. Biological seed characteristics of spring-emergence and autumn-emergence *Erodium oxyrhinchum*. Arid Zone Research, 37(06): 1562–1568. (in Chinese)

Li P M, Gao H Y, Strasser R J. 2005. Application of the fast chlorophyll fluorescence induction dynamics analysis in photosynthesis study. Physiology and Molecular Biology of Plants, 31(6): 559–566. (in Chinese)

Li P M. 2007. Application of chlorophyll *a* fluorescence transient in study of plant physiology under stress conditions. PhD Dissertation. Tai'an: Shandong Agricultural University. (in Chinese)

Li Y H, Liu J H, Zhao B P, et al. 2020. Effect of drought stress on oat growth and leaf photosystem II activity. Acta Botanica Boreali-Occidentalia Sinica, 40(10): 1706–1713. (in Chinese)

Lima C S, Ferreira-Silva S L, Carvalho F E L, et al. 2018. Antioxidant protection and PSII regulation mitigate photo-oxidative stress induced by drought followed by high light in cashew plants. Environmental and Experimental Botany, 149: 59–69.

Liu H L, Chen Y F, Zhang L W, et al. 2021. Is the life history flexibility of cold desert annuals broad enough to cope with predicted climate change? The case of *Erodium oxyrhinchum* in Central Asia. Biology, 10(8): 780, doi: 10.3390/biology10080780.

Liu J, Guo Y Y, Bai Y W, et al. 2018. Effects of drought stress on the photosynthesis in maize. Russian Journal of Plant Physiology, 65(6): 849–856.

Liu Z D, Ran Q Y, Chen Y, et al. 2018. Ecological effects of condensed water to ephemeral plants *Lappula semiglabra* in desert. Arid Zone Research, 35(6): 1290–1298. (in Chinese)

Lu J Z, Yin Z P, Lu T, et al. 2020. Cyclic electron flow modulate the linear electron flow and reactive oxygen species in tomato leaves under high temperature. Plant Science, 292: 110387, doi: 10.1016/j.plantsci.2019.110387.

Luo H H, Tsimilli-Michael M, Zhang Y L, et al. 2016. Combining gas exchange and chlorophyll *a* fluorescence measurements to analyze the photosynthetic activity of drip-irrigated cotton under different soil water deficits. Journal of Integrative Agriculture, 15(6): 1256–1266.

Ma L, Zhang Z H, Yao B Q, et al. 2021. Effects of drought and heat on the productivity and photosynthetic characteristics of alpine meadow plants on the Qinghai-Tibetan Plateau. Journal of Mountain Science, 18(8): 2079–2093.

Manaa A, Goussi R, Derbali W, et al. 2021. Photosynthetic performance of quinoa (*Chenopodium quinoa* Willd.) after exposure to a gradual drought stress followed by a recovery period. Biochimica et Biophysica Acta (BBA)-Bioenergetics, 1862(5): 148383, doi: 10.1016/j.bbabio.2021.148383.

Min X J. 2020. Photosynthetic response and growth adaptation strategies of desert herbaceous plants to rainfall variation. PhD Dissertation. Beijing: University of Chinese Academy of Sciences. (in Chinese)

Mu X H, Huang G, Li Y, et al. 2021. Population dynamics and life history response to precipitation changes for a desert ephemeral plant with biseasonal germination. Frontiers in Plant Science, 12: 625475, doi: 10.3389/fpls.2021.625475.

Paunov M, Koleva L, Vassilev A, et al. 2018. Effects of different metals on photosynthesis: cadmium and zinc affect chlorophyll fluorescence in durum wheat. International Journal of Molecular Sciences, 19(3): 787, doi: 10.3390/ijms19030787.

Pinheiro C, Chaves M M. 2011. Photosynthesis and drought: can we make metabolic connections from available data? Journal of Experimental Botany, 62(3): 869–882.

Platt T, Gallegos C L, Harrison W G. 1980. Photoinhibition of photosynthesis in natural assemblages of marine phytoplankton. Journal of Marine Research, 38(4): 687–701.

Qiu J, Tan D Y, Fan D Y. 2007. Characteristics of photosynthesis and biomass allocation of spring ephemerals in the Junggar Desert. Chinese Journal of Plant Ecology, 31(5): 883–891. (in Chinese)

Redillas M C F R, Strasser R J, Jeong J S, et al. 2011. The use of JIP test to evaluate drought-tolerance of transgenic rice overexpressing *OsNAC10*. Plant Biotechnology Reports, 5: 169–175.

Schreiber U, Schliwa U, Bilger W. 1986. Continuous recording of photochemical and non-photochemical chlorophyll fluorescence quenching with a new type of modulation fluorometer. Photosynthesis Research, 10(1–2): 51–62.

Shi S B, Li T C, Li M, et al. 2015. Interaction effect analysis of soil drought and strong light on PSII non-photochemical quenching in *Kobresia pygmaea* leaves. Plant Physiology Journal, 51(10): 1678–1686. (in Chinese)

Stirbet A, Govindjee. 2011. On the relation between the Kautsky effect (chlorophyll a fluorescence induction) and Photosystem

II: Basics and applications of the OJIP fluorescence transient. Journal of Photochemistry and Photobiology B: Biology, 104(1–2): 236–257.

Stirbet A, Govindjee. 2012. Chlorophyll *a* fluorescence induction: a personal perspective of the thermal phase, the J-I-P rise. Photosynthesis Research, 113(1): 15–61.

Strasser R J, Srivastava A, Govindjee. 1995. Polyphasic chlorophyll *a* fluorescence transient in plants and cyanobacteria. Photochemistry and Photobiology, 61(1): 32–42.

Strasser R J, Srivastava A, Tsimilli-Michael M. 2000. The fluorescence transient as a tool to characterize and screen photosynthetic samples. In: Yunus M, Pathre U, Mohanty P. Probing Photosynthesis: Mechanism, Regulation and Adaptation. London: Taylor and Francis Press, 445–483.

Strasser R J, Tsimilli-Michael M, Srivastava A. 2004. Analysis of the chlorophyll *a* fluorescence transient. In: Papageorgiou G C, Govindjee. Chlorophyll *a* Fluorescence. Advances in Photosynthesis and Respiration. Dordrecht: Springer, 321–362.

Strasser R J, Tsimilli-Michael M, Qiang S, et al. 2010. Simultaneous *in vivo* recording of prompt and delayed fluorescence and 820-nm reflection changes during drying and after rehydration of the resurrection plant *Haberlea rhodopensis*. Biochimica et Biophysica Acta-Bioenergetics, 1797(6–7): 1313–1326.

Talbi S, Rojas J A, Sahrawy M, et al. 2020. Effect of drought on growth, photosynthesis and total antioxidant capacity of the saharan plant *Oudeneya africana*. Environmental and Experimental Botany, 176: 104099, doi: 10.1016/j.envexpbot.2020.104099.

Tu W F, Li Y, Liu W, et al. 2016. Spring ephemerals adapt to extremely high light conditions via an unusual stabilization of photosystem II. Frontiers in Plant Science, 6: 1189, doi: 10.3389/fpls.2015.01189.

Vincent C, Schaffer B, Rowland D. 2018. Water-deficit priming of papaya reduces high-light stress through oxidation avoidance rather than anti-oxidant activity. Environmental and Experimental Botany, 156: 106–119.

Wang C, Gu Q L, Zhao L J, et al. 2022. Photochemical efficiency of photosystem II in inverted leaves of soybean [*Glycine max* (L.) Merr.] affected by elevated temperature and high light. Frontiers in Plant Science, 12: 772664, doi: 10.3389/fpls.2021.772644.

Wang F L, Chai C W, Zhao P, et al. 2021. Photosynthetic and chlorophyll fluorescence responses of three desert species to drought stress and evaluation of drought resistance. Acta Botanica Boreali-Occidentalia Sinica, 41(10): 1755–1765. (in Chinese)

Wang J W, Liu Y, Xu Y X, et al. 2022. Sexual differences in gas exchange and chlorophyll fluorescence of *Torreya grandis* under drought stress. Trees, 36: 283–294.

Wang W, Huang L N, Chen Q X. 2014. Rapid detection of photosynthetic capacity on cultivars of *Yellow phalaenopsis*. Subtropical Plant Science, 43(1): 4–7. (in Chinese)

Wang X Q, Jiang J, Wang Y C, et al. 2006. Responses of ephemeral plant germination and growth to water and heat conditions in the southern part of Gurbantunggut Desert. Chinese Science Bulletin, 51(Suppl. 1): 110–116.

Wang Z B, Li G F, Sun H Q, et al. 2018. Effects of drought stress on photosynthesis and photosynthetic electron transport chain in young apple tree leaves. Biology Open, 7(11): bio035279, doi: 10.1242/bio.035279.

Wilson S, Ruban A V. 2020. Enhanced NPQ affects long-term acclimation in the spring ephemeral *Berteroa incana*. Biochimica et Biophysica Acta-Bioenergetics, 1861(4): 148014, doi: 10.1016/j.bbabio.2019.03.005.

Wu L S, Zhang L, Tu W F, et al. 2020. Photosynthetic inner antenna CP47 plays important roles in ephemeral plants in adapting to high light stress. Journal of Plant Physiology, 251: 153189, doi: 10.1016/j.jplph.2020.153189.

Wu N, Zhang J, Wang Y, et al. 2018. Effects of snow cover and arbuscular mycorrhizal fungi network on the seedling growth of *Erodium oxyrrhynchum*. Arid Zone Research, 35(3): 624–632. (in Chinese)

Xu N, Meng X X Y, Zhao X M, et al. 2017. Responses of photosynthetic characteristics in leaves of *Physocarpus amurensis* and *P.opulifolius* to drought stress. Chinese Journal of Applied Ecology, 28(6): 1955–1961. (in Chinese)

Yuan S F, Tang H P. 2010a. Research advances in the eco-physiological characteristics of ephemerals adaptation to habitats. Acta Prataculturae Sinica, 19(1): 240–247. (in Chinese)

Yuan S F, Tang H P. 2010b. Patterns of ephemeral plant communities and their adaptations to temperature and precipitation regimes in Dzungaria Desert, Xinjiang. Biodiversity Science, 18(4): 346–354. (in Chinese)

Yue Z W, Li C D, Li L, et al. 2020. Responses of leaf morphology and fluorescence parameters of *Alhagi sparsifolia* in different light environments. Arid Zone Research, 37(3): 722–728. (in Chinese)

Zagorchev L, Traianova A, Teofanova D, et al. 2020. Influence of *Cuscuta campestris Yunck.* on the photosynthetic activity of *Ipomoea tricolor Cav.* - *in vivo* chlorophyll *a* fluorescence assessment. Photosynthetica, 58: 422–432.

Zhang L Y, Chen C D. 2002. On the general characteristics of plant diversity of Gurbantunggut Sandy Desert. Acta Ecologica Sinica, (11): 1923–1932. (in Chinese)

Zhang Y L, Yin B F, Tao Y, et al. 2022. Effects of the first rainfall timing and amount on morphological characteristics and chlorophyll fluorescence of two ephemeral species in the Gurbantünggüt Desert, northwestern China. Chinese Journal of Plant Ecology, 46(4): 428–439. (in Chinese)

Zhou R H, Kan X, Chen J J, et al. 2019. Drought-induced changes in photosynthetic electron transport in maize probed by prompt fluorescence, delayed fluorescence, P700 and cyclic electron flow signals. Environmental and Experimental Botany, 158: 51–62.

Zhou X B, Zhang Y M, Wang S S, et al. 2010. Combined effects of simulated nitrogen deposition and drought stress on growth and photosynthetic physiological responses of two annual desert plants in Junggar Basin, China. Chinese Journal of Plant Ecology, 34(12): 1394–1403. (in Chinese)

Zhuang W W, Zhang Y M. 2017. Effects of biological soil crusts on the photosynthetic characteristics of three desert herbs in Gurbantunggut Desert. Plant Science Journal, 35(3): 387–397. (in Chinese)

Zivcak M, Brestic M, Balatova Z, et al. 2013. Photosynthetic electron transport and specific photoprotective responses in wheat leaves under drought stress. Photosynthesis Research, 117(1–3): 529–546.